

## Deuteron-magnetic-resonance study of the cluster formation in the liquid and supercooled-liquid state of 2-cyclooctylamino-5-nitropyridine

R. Kind, O. Liechti, N. Korner, and J. Hulliger

*Eidgenössische Technische Hochschule Zürich-Hönggerberg, Institut für Quantenelektronik, CH-8093 Zürich, Switzerland*

J. Dolinsek and R. Blinc

*Jozef Stefan Institute, University of Ljubljana, YU-61111 Ljubljana, Slovenia*  
(Received 20 September 1991; revised manuscript received 12 November 1991)

The freezing behavior and the cluster formation in the liquid and supercooled-liquid state of mono-deuterated 2-cyclooctylamino-5-nitropyridine have been studied by deuteron magnetic resonance and relaxation. The results show that the molecular dynamics is both polydispersive and non-Arrhenius-like. The data can be described by a correlation function of the stretched-exponential type and a Vogel-Fulcher-type temperature dependence of the mean correlation times. The existence of polydispersity already in the liquid state may be interpreted in terms of molecular clusters of different sizes. The mean size of these clusters and their temperature dependence have been estimated by a combination of deuteron NMR and proton self-diffusion data. Nonlinear-optical data further suggest that molecular chains in the clusters are arranged in an antiparallel manner.

### I. INTRODUCTION

In recent years the interest in using purely organic crystals of donor- and acceptor-substituted delocalized  $\pi$ -electron systems for laser optics has increased considerably because of their strong nonlinear-optical (NLO) susceptibilities.<sup>1</sup> In view of the increasing interest in the formation of molecular glasses (i.e., locally ordered states that have to be classified between a crystalline solid and a randomly "frozen-out" supercooled liquid) and in the corresponding cluster formation and molecular dynamics, the question about the melting and solidification behavior of organic systems with NLO properties also becomes of great importance. Especially the possible formation of polar glasses<sup>2</sup> with similar NLO properties, as reported for some polymers,<sup>3</sup> will be a goal of future investigations. It has been known for a long time that some organic compounds form extremely stable supercooled liquid states<sup>4,5</sup> (e.g., De Coppet<sup>6</sup> has shown that melts of salol, as well as Glauber salt solutions, could be kept for more than 35 years in the supercooled-liquid state).

One of these compounds exhibiting interesting NLO properties is 2-cyclooctylamino-5-nitropyridine (COANP). It has recently been investigated in its crystalline state by a series of NLO experiments.<sup>7</sup> These investigations became possible because of a recent breakthrough in the crystal growth of this material. The most successful method, which yielded large crystals of optical quality was growth from the supercooled melt.<sup>8</sup> While elaborating the proper growth conditions we became aware of a solidification behavior that can be characterized as follows: Chemically pure, (almost) dust free, superheated COANP melts do not show crystallization upon cooling below the melting point at cooling rates that are typical for differential scanning calorimetry (DSC) experiments (1–20 K/min). Even further cooling to much lower tem-

peratures will not lead to crystallization. Upon consecutive heating, the material remains in a quasiwaxlike glassy state up to about 40–20 K below the melting temperature  $T_m$  where it crystallizes completely within a short time.<sup>9</sup> Upon further increasing the temperature, the system melts at the nominal fusion temperature of  $T_m = 72.8 \pm 0.1^\circ\text{C}$ . This scenario seems to be fairly common in molecular glass formers. Early work on the nucleation of classical organic systems<sup>10</sup> revealed the existence of two distinct and only weakly overlapping temperature regions where the nucleation rate or the crystal-growth rate (which is strongly related to the translational diffusion), respectively, are maximum. In contrast to the DSC scans, experiments connected with the bulk growth of COANP revealed that sufficiently slow cooling of superheated melts to a temperature, which is not lower than 5–10 K below  $T_m$ , exhibits spontaneous nucleation after some time (hours to days). This can be explained by the fact that the temperature region, where the diffusion is high enough for crystallization, lies above the region for maximum nucleation rate, so that for the DSC-cooling scans from the superheated melt we first have a lack of nucleation centers followed by an insufficient diffusion for crystallization.<sup>11</sup> A crucial question is, whether the system remains in this completely disordered state or whether it undergoes a phase transition to a nonergodic thermodynamic state, which corresponds to a structural glass. DSC scans showed a small anomaly in the specific heat of COANP at 263 K. At this temperature, which is referred to as glass temperature  $T_g$ , the re-orientational part of the dielectric relaxation becomes infinitely long. This has been observed recently in second-harmonic-generation experiments on poled, supercooled COANP.<sup>2</sup>

In order to gain more information on the nature of the supercooled state of COANP and of a possibly glassy

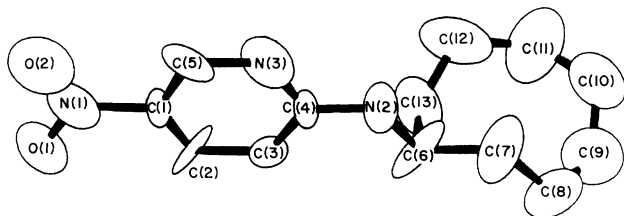


FIG. 1. Basic structure of the COANP molecule after Ref. 7. The proton positions are not shown. The molecule was deuterated at the secondary amine N2.

state of this system, we have performed a series of proton NMR line-shape,  $T_1$ -dispersion, and diffusion measurements. The analysis of the data has failed in so far that it was not possible to explain all data with the same relaxation mechanism and also the introduction of a Kohlrausch-Williams-Watts (KWW) function ( $\exp[-(t/\tau_0)^\alpha]$ ) for the single-particle autocorrelation function yielded contradictory results on the distribution function of autocorrelation times.

At this point we decided to simplify the analysis by partial deuteration of the molecules. In fact there is only one out of the 19 protons that exchanges easily in the solution: The proton that forms a bond with the secondary amine N(2), Fig. 1.<sup>7</sup> In the crystalline phase this proton forms a N—H  $\cdots$  O hydrogen bridge to the O(2) of the nitro group of an adjacent molecule. The advantage of NMR on the deuteron in this position is that all intra- and intermolecular interactions messing up the proton NMR can be neglected. We have to deal only with the behavior of the corresponding quadrupole perturbed Zeeman Hamiltonian of the deuterons under the influence of motion.

## II. SAMPLE PREPARATION

COANP powder material for crystal growth and melt studies was synthesized as outlined in Ref. 7. The substitution of the proton at the secondary amine N—H bond (see Fig. 1) by a deuteron was then achieved by repeated precipitation of the COANP deuteriochloride in a mixture of DCl, D<sub>2</sub>O, and CH<sub>3</sub>—CH<sub>2</sub>—OD. The resulting deuterio-COANP was recrystallized from a toluene-isooctane solution. The sample for the NMR measurements was sealed in a glass tube, which was always heated above  $T_m$  before any measurement took place, in order to remove the crystalline phase completely. For comparison we wanted to determine also the deuteron EFG tensor in the crystalline phase. For this purpose a single crystal was grown from supercooled melt at  $T_m - T \approx 0.3$ – $0.5$  K. This method yielded similar triangular crystal plates as reported already for ordinary COANP.<sup>8</sup> The sample used for the NMR experiments had the dimensions of  $3 \times 3 \times 8$  mm.<sup>3</sup>

## III. EXPERIMENTAL

The deuteron NMR signal of the supercooled deuterio-COANP was measured on a home built pulsed NMR

spectrometer in an external magnetic field of 7 T ( $\nu_L = 46.05$  MHz). The line shape was obtained by a Fourier transform of the spin echo of a  $90_x - \tau - 90_y$  pulse sequence. On lowering the temperature  $T$  from the liquid phase, the narrow Lorentzian signal (HWHH  $\approx 90$  Hz, which is typical for motional averaging) broadens out and finally ends below room temperature in a broad powder pattern indicating a static quadrupolar coupling of  $e^2qQ/h = 200$  kHz with an asymmetry parameter  $\eta = 0.15$ , Fig. 2. The narrow line in the center of the powder pattern is an artifact originating from the ringing of the resonance circuit.

The transverse relaxation time  $T_2$  was determined from the fit of a Lorentzian  $1/[1+(\delta\omega T_2)^2]$  to the motionally narrowed homogeneous signal shape  $g(\omega, T)$ . The inhomogeneity of the static magnetic field was determined in a separate experiment with deuteron magnetic resonance (DMR) of D<sub>2</sub>O in an identical sample tube to be of almost Gaussian shape with a standard deviation  $\sigma = 2\pi \times 62$  Hz. The homogeneous signal shape was obtained from a deconvolution of the measured signal.

The longitudinal relaxation time  $T_1$  was determined from the magnetization recovery  $M(\tau)$  of the free-induction decay in a  $90_x - \tau - 90_x$  pulse sequence. It was measured at two different Larmor frequencies 41.44 and 13.3 MHz, respectively, in a temperature range from 37 to 120°C.  $M(\tau) - M_0$  showed a precise exponential decay for the whole temperature range. In Fig. 3  $\ln(T_1)$  and  $\ln(T_2)$  are displayed as a function of the inverse temperature  $1/T$ .

The EFG tensor in the crystalline phase was determined from a single-crystal DMR rotation pattern where the crystal was rotated about an axis close to the  $c$  axis. According to the space group  $Pca2_1$  with  $Z = 4$ , the rotation pattern revealed four pairs of lines that are related

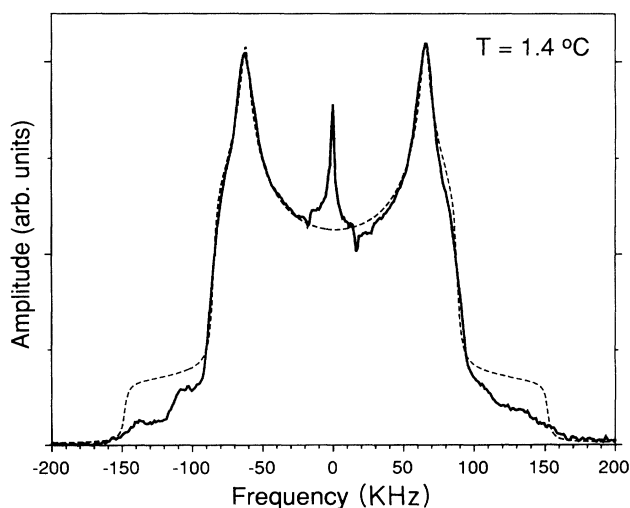


FIG. 2. DMR spectrum of deuterio-COANP at 274.7 K for  $\nu_L = 46.1$  MHz, (solid line). The dashed line is calculated from a fit with the parameters  $e^2qQ/h = 200$  kHz and  $\eta = 0.15$ . The peak in the center of the spectrum is an artifact originating from the ringing of the resonance coil.

by the point symmetry of the crystal. The nonlinear fit procedure revealed also a quadrupole coupling constant of  $e^2qQ/h=200$  kHz with  $\eta=0.16$ , in good agreement with the values obtained from the supercooled liquid cooling experiment.

#### IV. THEORY

The relaxation rates  $1/T_1$  and  $1/T_2$  for a static nuclear-quadrupole (NQ) Hamiltonian of a spin  $I=1$ , in a high magnetic field, for the case of isotropic rotational diffusion are common knowledge in the field of NMR.<sup>12</sup>

$$\frac{1}{T_1} = \frac{3}{80} \left[ \frac{e^2qQ}{\hbar} \right]^2 \left[ 1 + \frac{\eta^2}{3} \right] [J(\omega_L) + 4J(2\omega_L)] \quad (1)$$

and

$$\frac{1}{T_2} = \frac{3}{160} \left[ \frac{e^2qQ}{\hbar} \right]^2 \left[ 1 + \frac{\eta^2}{3} \right] \times [3J(0) + 5J(\omega_L) + 2J(2\omega_L)], \quad (2)$$

where  $J(0)$ ,  $J(\omega_L)$ , and  $J(2\omega_L)$  are the fluctuation spectral densities at the frequencies zero,  $\omega_L$ , and  $2\omega_L$ , respectively. The spectral densities are the Fourier transform of the normalized autocorrelation function  $G(t)$  of the fluctuations of the EFG tensor elements in the laboratory frame,

$$J(\omega) = \int_0^\infty dt \cos(\omega t) G(t). \quad (3)$$

In the case of a monodisperse relaxation, where  $G(t) = \exp(-t/\tau_c)$  this integral can be solved analytically and yields the well-known relation

$$J(\omega) = \frac{\tau_c}{1 + \omega^2\tau_c^2}, \quad (4)$$

whereas for a polydisperse relaxation, numerical integration has to be used in most cases. A typical example for a polydisperse relation is the KWW function  $G(t) = \exp[-(t/\tau_0)^\alpha]$ , where  $\alpha$  is the so-called stretched exponent ( $0 < \alpha < 1$ ). It is polydisperse because it can be expressed by a distribution  $\rho(\tau_c)$  of exponential decays.<sup>13</sup> For this autocorrelation function one can calculate the spectral densities analytically for the extreme fast-motion regime ( $\omega\tau_c \ll 1$ ) and in the extreme slow-motion regime ( $\omega\tau_c \gg 1$ ):

$$J(\omega) = \Gamma \left[ \frac{1}{\alpha} + 1 \right] \tau_0$$

and

$$J(\omega) = \frac{\Gamma(\alpha+1) \sin(\pi\alpha/2)}{\omega^{\alpha+1} \tau_0^\alpha}, \quad (5)$$

respectively. Here  $\Gamma$  stands for the complete  $\Gamma$  function. Expression (5) yields for  $\alpha=1$  the same values as Eq. (4) for the two extreme cases. As mentioned above, the spectral densities for the range

$$0.2 \exp(-1/\alpha) < \omega\tau_0 < 5 \exp(1/\alpha)$$

can be obtained from numerical integration only.

It should be noted that  $J(0)$ , as well as  $J(\omega)$  in the extreme fast motion regime, are given just by the area under  $G(t)$ . This means that from a  $T_2$  measurement in the extreme narrowing regime, as well as from a  $T_1$  measurement in the fast-motion regime, no information about the decay of  $G(t)$ , or  $\rho(\tau_c)$ , respectively, can be obtained. In contrast to the fast-motion regime, the shape of  $G(t)$  is of a certain importance in the slow-motion regime, since it affects the slope, as well as the dispersion of  $T_1$ . This is demonstrated for the case of the KWW function in Eqs. (5). It needs, however, very precise measurements over several orders of magnitude of  $\tau_c$  to allow for an unambiguous determination of the distribution function  $\rho(\tau_c)$ . Because of this we have used only the KWW function for the data analysis though other models have been proposed for the autocorrelation function  $G(t)$ .<sup>14</sup>

According to Ref. 12, the Lorentzian linewidth  $\delta$  (HWHH) in the extreme narrowing case is given by

$$\delta = \langle \omega_p^2 \rangle \tau' = \int_{-\infty}^{+\infty} \omega^2 g(\omega) d\omega \int_0^\infty G(\tau) d\tau, \quad (6)$$

i.e., it corresponds to the second moment of the rigid lattice line shape, times the spectral density  $J(0)$ . The rigid lattice line shape  $g(\omega)$  of randomly oriented EFG tensors in the high-field case ( $I=1$ ,  $\eta=0$ ) is given by a Pake pattern of the form

$$g(\omega) = \frac{1}{2[3(2\omega\omega_q + \omega_q^2)]^{1/2}} + \frac{1}{2[3(-2\omega\omega_q + \omega_q^2)]^{1/2}}, \quad (7)$$

where  $\omega_q = \frac{3}{4}(e^2qQ/\hbar)$ . The second moment of  $g(\omega)$  amounts to  $\omega_q^2/5$ , so that the Lorentzian linewidth (HWHH) is given by

$$\delta = \frac{3}{160} \left[ \frac{e^2qQ}{\hbar} \right]^2 3J(0). \quad (8)$$

This corresponds exactly to the secular part of  $1/T_2$  for  $\eta=0$ , so that the relation  $T_2=1/\delta$  holds as long we are in the extreme narrowing regime, i.e., for  $\delta \ll \omega_q$ . It should be noted that Eq. (6) was derived for a Gaussian  $g(\omega)$  but it seems to hold in the extreme narrowing regime also for other frequency distributions. In the neighborhood of the  $T_1$  minimum and in the fast-motion regime,  $\delta$  is affected by  $T_1$  effects in the same way as  $1/T_2$ , i.e., when the nonsecular parts become of importance in Eq. (2).

A crucial problem is the relation between the temperature  $T$  and the average autocorrelation time  $\tau_0$ . While the autocorrelation time of uncorrelated thermally activated motions is well described by the Arrhenius law,  $\tau_c = \tau_\infty \exp(E_a/k_B T)$ , where  $E_a$  is the barrier height and  $\tau_\infty$  the inverse attempt frequency, this is rarely the case when the motions become correlated due to the formation of clusters. In such cases the Vogel-Fulcher modification of the Arrhenius law  $\tau_c = \tau_\infty \exp[E_a/k_B(T-T_0)]$ —which is of entirely empirical nature—seems to describe the temperature dependence of  $\tau_c$  quite well, at least within a certain tem-

perature range well above  $T_0$ . In order to prove or disprove the Arrhenius behavior, the experimental data of a  $T_1$  or  $T_2$ , measurements are usually plotted in a logarithmic scale versus  $1/T$ , i.e., versus  $\ln(\tau_c)$  for the case the Arrhenius law holds. It can easily be seen from Eqs. (4) and (5) that one has to expect, for this case, a straight line with a negative slope, which is proportional to  $E_a$  in the fast-motion regime, whereas in the slow-motion regime one should observe a straight line with a positive slope proportional to  $\alpha E_a$ . This holds, however, only far enough from the  $T_1$  minimum.

In the  $T_1$  minimum the relaxation does not depend on the temperature and thus not on the average autocorrelation time  $\tau_0$ . It depends only on the mean-square amplitudes of the fluctuations, on the Larmor frequency  $\omega_L$ , and on the stretched exponent  $\alpha$ , i.e., on the distribution function of the autocorrelation times. This allows for an unambiguous determination of  $\tau_0$  (which lies somewhere between  $1/\omega_L$  and  $1/2\omega_L$  depending on the distribution function of  $\tau_c$  at the temperature), as well as the relation between the mean fluctuation amplitude and  $\alpha$ . If the mean fluctuation amplitude is known, as in our case where the local static EFG tensor at the deuteron site is known, the value of  $T_1$  in the minimum allows for a determination of  $\alpha$ .

Another question that might be of importance is the influence of the anisotropy in the rotational diffusion. This is so as the COANP molecule does not have a spherical shape but has a more rodlike structure with a short and two long axes in the ellipsoid of inertia. The problem of NMR relaxation due to anisotropic rotational diffusion is treated in great detail in Ref. 15. Evaluations of the corresponding equations showed that the value of the  $T_1$  minimum is almost not affected, even in the case of rather strong anisotropy in the rotational diffusion. However, the single-particle autocorrelation time depends on the relative orientation between the interaction tensor (here the EFG tensor at the deuteron site) and the rotational diffusion tensor of the molecule, but the effect is limited to a factor of about 0.5–2.

## V. DISCUSSION

The solid lines in Fig. 3 are the result of a simultaneous BPP fit (monodispersive, Arrhenius valid) to the  $T_1$  data at  $\nu_L = 41.1$  MHz and  $\nu_L = 13.3$  MHz. The resulting fit parameters are  $e^2qQ/h = 156$  kHz,  $E_a = 0.571$  eV,  $\tau_\infty = 1.16 \times 10^{-17}$  s. The asymmetry parameter was kept constant at  $\eta = 0.15$ . One can see that the fitted quadrupole coupling constant is well below the static value of  $e^2qQ/h = 200$  kHz obtained from the Pake pattern, Fig. 2. Furthermore, the  $T_2$  values calculated for these parameters for  $\nu_L = 46.1$  MHz (dashed line in Fig. 3) differ by a factor up to 24 from the measured values. This clearly shows, according to Eqs. (5), that either  $\tau_0(T)$  is not of Arrhenius type, or the system is not monodispersive ( $\alpha < 1$ ), or both.

The first of these possibilities (non-Arrhenius, but monodispersive) can be ruled out rather easily. If the  $\tau_0(T)$  scale is changed in such a way that the calculated

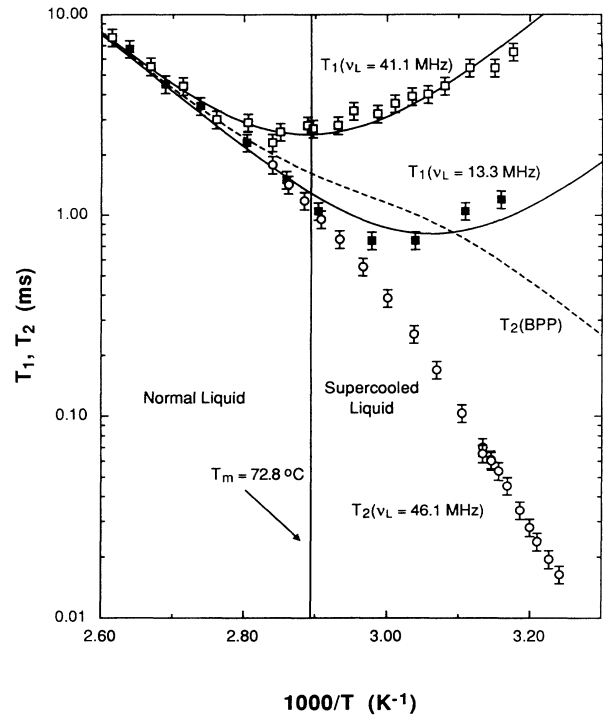


FIG. 3. DMR spin-lattice relaxation  $T_1$  at 41.1 MHz (open squares) and at 13.3 MHz (closed squares), and transverse DMR relaxation  $T_2$  at 46.1 MHz (open circles) vs inverse temperature  $1000/T$ . The solid lines are calculated from a simultaneous BPP fit of both  $T_1$  data sets. The dashed line represents the calculated  $T_2$  using the parameters of the  $T_1$  fit.

$T_2$  values match the measured ones, the error is just transferred to the calculated  $T_1$  values of the slow-motion regime, since  $T_2$  is proportional to  $1/\tau_c$ , whereas  $T_1$  is proportional to  $\tau_c$  in the slow-motion regime. Furthermore, in order to match the  $T_1$  values in the minima with the measured static  $e^2qQ/h = 200$  kHz, the value of the stretched exponent  $\alpha$  must be reduced from 1.0 to 0.55.

The second possibility [Arrhenius for  $\tau_0(T)$ , but polydispersive] is not so easy to rule out with the present data, since quite reasonable fits can be obtained for both temperature-dependent and temperature-independent  $\alpha$ , though in the latter case rather unrealistic fit parameters were obtained ( $E_a = 1$  eV,  $\tau_\infty = 5 \times 10^{-24}$  s). We know, however, from our proton  $T_1$  and  $T_2$  measurements that this possibility does not lead to satisfactory results. Moreover, Eich *et al.*<sup>2</sup> have observed a strong departure from the Arrhenius behavior of the characteristic time for the reorientation of the electric dipoles in COANP by means of dielectric and second-harmonic measurements. We are thus left with the last possibility: Both non-Arrhenius and polydispersive. A similar behavior has recently been observed in poly(vinyl acetate) above the glass transition temperature by means of multidimensional NMR.<sup>16</sup>

There are two ways to account for the non-Arrhenius behavior of  $\tau_0(T)$ : (a) to use a temperature-dependent en-

ropy of activation  $\Delta S_a(T)$  or (b) a temperature-dependent activation energy  $E_a(T)$ . This last approach leads in the case of glasses usually to a Vogel-Fulcher modification of the Arrhenius law. Since the  $\tau(T)$  data extracted from Ref. 2 can be fitted with a Vogel-Fulcher ansatz with  $E_a = 83.2$  meV,  $\tau_\infty = 1.03 \times 10^{-12}$  s and  $T_0 = 239$  K over ten orders of magnitude in the time scale, we have used this information for our calculations. It should be noted that the fitted Vogel-Fulcher temperature  $T_0$  is about 24 K below the glass temperature  $T_g = 263$  K mentioned in the introduction. Together with our known data ( $e^2 q Q / h = 200$  kHz,  $\eta = 0.15$ , and  $\alpha = 0.55$ ), but with an inverse attempt frequency  $\tau_\infty = 1.8 \times 10^{-13}$  s, which is by a factor of 6, shorter than obtained from the dielectric measurements, we obtained an almost perfect agreement with our measured data, Fig. 4. This factor of 6 can be explained in the following way: From the theory for rotational diffusion,<sup>12,15</sup> it follows that the autocorrelation time is proportional to  $1/l(l+1)$  in connection with the expansion of the probability function  $\Psi(\Omega, t)$  into spherical harmonics. In dielectric measurements one observes an  $l=1$  effect, whereas in the NMR relaxation we have  $l=2$ . This accounts already for a factor of 3 between the two correlation times. The remaining factor of 2 is probably due to the anisotropic rotational diffusion. In the COANP molecule the electric dipole moment points along the long axis of the molecule, whereas the principal  $z$  axis of the deuteron EFG tensor is almost perpendicular to it. It is therefore plausible that the anisotropy of the rotational

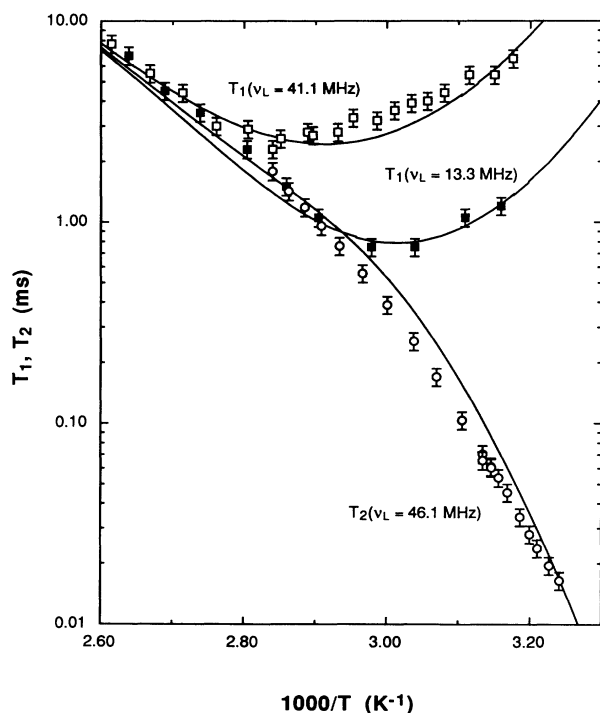


FIG. 4. Same measured data as in Fig. 3. The solid lines are calculated with a set of parameters that describe a polydisperse non-Arrhenius type of reorientational motion.

diffusion affects the corresponding correlation times in a different way. However, the accuracy of both the extracted data of Ref. 2 and of our measurements are not sufficient to allow for a quantitative analysis of this effect.

The fact that the rotational diffusion of the COANP system is of polydisperse nature already in the liquid state may be interpreted in terms of molecular clusters of different sizes in both the liquid and the supercooled-liquid state. If this is the case, the critical question is, whether we can derive information concerning the size and the nature (order of the molecules in the body and on the surface) of these clusters from our data. The existence of molecular clusters would imply that a great part of the N—H · · · O bonds are not broken on going from the crystalline to the liquid phase as in the case of percolation. This means that we would observe the reorientation of whole clusters rather than of single molecules. In the following, we shall assume the existence of such molecular clusters, though we are well aware that there are other possible interpretations for the polydispersity of the motion.

For the liquid phase we assume that the diffusion equation, as well as the Stokes-Einstein formulas for the translational and rotational diffusion constants  $D$  and  $D_s$ , respectively, are valid:

$$D = \frac{k_B T}{6\pi a \eta}, \quad D_s = \frac{k_B T}{8\pi a \eta}, \quad D = \frac{4}{3} D_s, \quad (9)$$

where  $a$  is the radius of a rigid macroscopic or microscopic sphere moving in a medium of viscosity  $\eta$ . The solution of the equation for rotational diffusion yields for the autocorrelation time  $\tau_2$ , which is relevant for NMR relaxation,

$$\tau_2 = \frac{a^2}{6D_s} = \frac{2a^2}{9D}, \quad \text{or } a = \left( \frac{9}{2} D \tau_2 \right)^{1/2}. \quad (10)$$

With this relation we can evaluate the average cluster size in the rigid sphere approximation, as well as the average number of molecules belonging to a cluster. The translational diffusion constant  $D$  is known from proton NMR diffusion measurements for the temperature range 58–110°C,<sup>17</sup> whereas  $\tau_2$  corresponds to our  $\tau_0$ . The resulting cluster size is shown in Fig. 5. One can see that the average number of molecules per cluster is increasing from 2 to 6 on lowering the temperature from 120 to 80°C. However, below this temperature the Stokes-Einstein equation seems to break down, since it is not reasonable that the cluster size would become smaller again at lower temperatures. The dashed line shows an extrapolation to lower temperatures that is certainly more reasonable than the drop of the solid line. The breakdown of the Stokes-Einstein equation is due to the divergence of the inverse translational diffusion constant  $D$  at 58°C.<sup>17</sup> A similar breakdown of the Stokes-Einstein relations (below a temperature  $T_c$  but well above  $T_g$ ) has been reported recently for several supercooled glass forming liquids.<sup>18</sup> It would be very useful to know more about the cluster size below 60°C, and an extrapolation (with the same second-order polynomial as used for the calculation of the dashed line) down to  $T_g = -10^\circ\text{C}$  yields 38

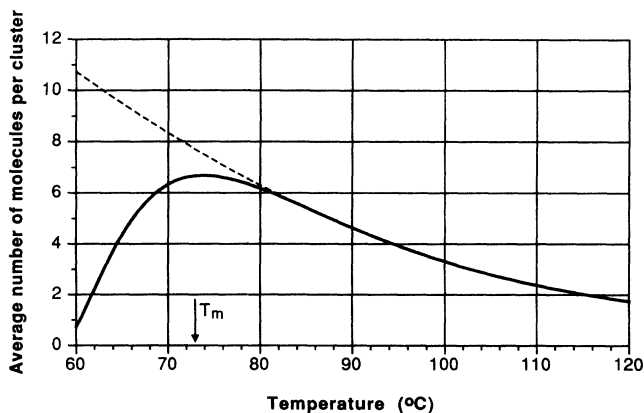


FIG. 5. Average number of COANP molecules forming a cluster vs temperature as derived from Eq. (10).

molecules per cluster, which might give an idea but is certainly a rather doubtful value.

Another interesting question concerns the local order within the clusters (always under the assumption that they exist). The fact that Eich *et al.*<sup>2</sup> could pole COANP in the supercooled state by applying an electric field, and observe second-harmonic-generation (SHG), shows that the clusters must be polar, i.e., the molecular dipoles must be arranged in such a way that the clusters carry a resulting dipole moment. Since the hyperpolarizability tensor  $\beta_{ijk}(-2\omega, \omega, \omega)$  of the COANP molecule has virtually only the element  $\beta_{zzz}$  different from zero, the nonlinear optical coefficient  $d_{33}$  is proportional to  $\langle \cos(\theta_l)^3 \rangle$ , where  $\theta_l$  is the angle between the donor-acceptor direction of the  $l$ th molecule and the electric-field direction of the incident wave of frequency  $\omega$ .<sup>19</sup> This fact allows for an estimation of the molecular order in poled supercooled COANP from the  $d_{33}$  values of the crystalline and the supercooled states. While the nonlinear optical coefficient for a perfect COANP single crystal was found to be  $d_{33} = 19$  pm/V,<sup>20</sup> the saturation value in the supercooled state around 0°C is found to be about 2.5 times smaller,  $d_{33} = 7.5$  pm/V.<sup>2</sup>

In the crystalline phase (space group  $Pca2_1$ ) the COANP molecules form infinite hydrogen bonded zig-zag chains (zig-zag angle between the electric dipoles equals 133°), which are aligned in layers perpendicular to the  $a$  axis. The direction of the chains alters from layer to layer and is either parallel to the  $(\mathbf{b} + \mathbf{c}/2)$  direction or to the  $(-\mathbf{b} + \mathbf{c}/2)$  direction, respectively [and not as erroneously stated in Ref. 7 ( $\pm \mathbf{b} + \mathbf{c}$ )]. The chains are thus tilted by an angle of 60.0° with respect to the polar crystal axis. Furthermore, the donor-acceptor axes of all COANP molecules are tilted by an angle of 61° with respect to the polar crystal axis. This results in a nonlinear optical coefficient  $d_{33}$ , which is by a factor of 8.9 smaller than for the hypothetical case where all COANP dipoles were aligned in the polarization direction of the incident optical beam of frequency  $\omega$ . A possible ex-

planation (but certainly not the only one) of the fact that the measured saturation value of  $d_{33}$  in the supercooled state is even by a factor of 22 smaller than this hypothetical value, is the absence of free reorientable COANP molecules in this phase. If all the chains could be aligned along the  $c$  axis then the tilt angle of the dipoles would be 23.8° and the resulting  $d_{33}$  still by a factor of 6.8 larger than the single-crystal value, which was not observed. Thus there are very likely no free reorientable COANP chains either. The most probable reason for the small value of  $d_{33}$  is an antiparallel arrangement of COANP chains of different lengths. The antiparallel arrangement cannot be removed by means of the external electric field. In order to gain more information on this ordering problem electric field induced second-harmonic saturation experiments should be performed as a function of temperature from the liquid phase down to  $T_g$ , since higher SHG efficiencies are to be expected in the liquid phase above 130°C, provided that our cluster model is true.

## VI. CONCLUSIONS

From the above results the following conclusions can be reached: (i) The molecular dynamics of COANP in the liquid and supercooled-liquid states is both polydispersive and non-Arrhenius far above the glass transition  $T_g$ . This is in sharp contrast to what is normally found in non-glass-forming liquids. (ii) The deuteron NMR data can be described by a correlation function of the stretched exponential type  $G(t) = \exp[-(t/\tau_0)^\alpha]$  and a Vogel-Fulcher type temperature dependence of the molecular reorientational correlation times  $\tau_0 = \tau_\infty \exp[E_a/k_B(T - T_0)]$ . The Vogel-Fulcher temperature  $T_0 = 239$  K is about 24 K below the glass transition temperature  $T_g$  as determined from thermal data. The activation energy is  $E_a = 83.2$  meV and  $\tau_\infty = 1.8 \times 10^{-13}$  s, which are very reasonable values for such a molecular liquid. (iii) The existence of polydispersity already in the liquid state may be interpreted in terms of molecular clusters. The mean size of these clusters can be estimated by a combination of deuteron NMR and proton self-diffusion data. According to this estimation the average cluster size would increase from 2 to 6 on lowering the temperature from 120 to 80°C. (iv) The comparison of the above data with the optical second-harmonic-generation data further suggest that chains of COANP molecules are probably arranged in an antiparallel way in the clusters, so that the total electric dipole moments are considerably reduced, as well as the SHG efficiency.

## ACKNOWLEDGMENTS

The authors would like to thank M. Ehrensperger for the synthesis and the preparation of the deuterated COANP. This work was supported in part by the Swiss National Science Foundation and the Research Community of Slovenia.

- <sup>1</sup>See, e.g., *Nonlinear Optical Properties of Organic Molecules and Crystals*, edited by D. S. Chemla and J. Zyss (Academic, New York, 1987), Vols. 1 and 2.
- <sup>2</sup>M. Eich, H. Looser, D. Y. Yoon, R. J. Twieg, G. Bjorklund, and J. C. Baumert, *J. Opt. Soc. Am. B* **6**, 1590 (1989).
- <sup>3</sup>See, e.g., *Nonlinear Optical Effects in Organic Polymers*, Vol. 162 of NATO *Advanced Studies Institutes, Series E: Applied Sciences*, J. Messier, F. Kajzar, P. Prasad, and D. Ulrich (Kluwer Academic, London, 1989).
- <sup>4</sup>N. B. Sing, M. E. Glicksman, and R. Mazelsky, *Prog. Crystal Growth Charact.* **17**, 265 (1988).
- <sup>5</sup>R. S. Tipson, in *Techniques of Organic Chemistry*, edited by A. Weissberger, (Interscience, New York, 1966), Vol. III, Pt. I, p. 395.
- <sup>6</sup>L. C. de Coppet, *Ann. Chim. Phys.* **10**, 457 (1907).
- <sup>7</sup>P. Günter, Ch. Bosshard, H. Arend, G. Chapuis, R. J. Twieg, and D. Dobrowolski, *Appl. Phys Lett.* **50**, 486 (1987); Ch. Bosshard, K. Sutter, P. Günter, and G. Chapuis, *J. Opt. Soc. Am. B* **6**, 721 (1989).
- <sup>8</sup>J. Hulliger, B. Brezina, and M. Ehrensperger, *J. Cryst. Growth* **106**, 605 (1990).
- <sup>9</sup>M. Ehrensperger, R. Kind, R. Blinc, and G. Lahajnar (unpublished).
- <sup>10</sup>K. Th. Wilke and J. Bohm, *Kristallzüchtung* (Deutsch, Frankfurt, 1988), and references therein.
- <sup>11</sup>A. Neuhaus, *Chem. Ing. Tech.* **28**, 155 (1956).
- <sup>12</sup>See, e.g., A. Abragam, *The Principles of Nuclear Magnetism* (Clarendon, Oxford, 1961).
- <sup>13</sup>E. Helfand, *J. Chem. Phys.* **78**, 1931 (1983).
- <sup>14</sup>W. Götze and L. Sjörgen, *J. Phys. C* **21**, 3407 (1988).
- <sup>15</sup>See, e.g., H. W. Spiess, in *NMR 15 Basic Principles and Progress*, edited by P. Diehl, E. Fluck, and R. Kosfeld (Springer-Verlag, Berlin, 1978), p. 128 ff. and references cited therein.
- <sup>16</sup>K. Schmidt-Rohr and H. W. Spiess, *Phys. Rev. Lett.* **66**, 3020 (1991).
- <sup>17</sup>R. Blinc, G. Lahajnar, I. Zupancic, R. Kind, J. Hulliger, and P. Günter, *Europhys. Lett.* (to be published).
- <sup>18</sup>E. Rössler, *Phys. Rev. Lett.* **65**, 1595 (1990).
- <sup>19</sup>D. Pugh and J. Ö. Morley, in *Nonlinear Optical Properties of Organic Molecules and Crystals*, edited by D. S. Chemla and J. Zyss (Academic, New York, 1987), Vol. 1, p. 193 ff.
- <sup>20</sup>Ch. Bosshard, Ph.D. thesis, Eidgenössische Technische Hochschule, 1991.